Journal of Hazardous Materials 180 (2010) 50–62

Contents lists available at ScienceDirect

Journal of Hazardous Materials

journal homepage: www.elsevier.com/locate/jhazmat

Evaluation of processes controlling the geochemical constituents in deep groundwater in Bangladesh: Spatial variability on arsenic and boron enrichment

M.A. Halim[a,b,*], R.K. Majumder[a], S.A. Nessa[b], Y. Hiroshiro[b], K. Sasaki[b], B.B. Saha[c], A. Saepuloh[d], K. Jinno[b]

[a] Isotope Hydrology Division, INST, Bangladesh Atomic Energy Commission, Savar, GPO Box-3787, Dhaka-1000, Bangladesh
[b] Institute of Environmental Systems, Graduate School of Engineering, Kyushu University, 744 Motooka, Nishi-ku, Fukuoka 819-0395, Japan
[c] Mechanical Engineering Department, National University of Singapore, 9 Engineering Drive 1, Singapore 117576, Singapore
[d] Department of Life and Environmental Sciences, Kumamoto University, Kurokami 2-39-1, Kumamoto 860-8555, Japan

ARTICLE INFO

Article history:
Received 18 November 2009
Received in revised form
30 December 2009
Accepted 4 January 2010
Available online 11 January 2010

Keywords:
Deep groundwater
Geochemical constituents
Arsenic
Boron
Geochemical model
Principal component analysis

ABSTRACT

Forty-six deep groundwater samples from highly arsenic affected areas in Bangladesh were analyzed in order to evaluate the processes controlling geochemical constituents in the deep aquifer system. Spatial trends of solutes, geochemical modeling and principal component analysis indicate that carbonate dissolution, silicate weathering and ion exchange control the major-ion chemistry. The groundwater is dominantly of Na–Cl type brackish water. Approximately 17% of the examined groundwaters exhibit As concentrations higher than the maximum acceptable limit of 10 μg/L for drinking water. Strong correlation ($R^2 = 0.67$) of Fe with dissolved organic carbon (DOC) and positive saturation index of siderite suggests that the reductive dissolution of Fe-oxyhydroxide in presence of organic matter is considered to be the dominant process to release high content of Fe (median 0.31 mg/L) in the deep aquifer. In contrast, As is not correlated with Fe and DOC. Boron concentration in the 26% samples exceeds the standard limit of 500 μg/L, for water intended for human consumption. Negative relationships of B/Cl ratio with Cl and boron with Na/Ca ratio demonstrate the boron in deep groundwater is accompanied by brackish water and cation exchange within the clayey sediments.

1. Introduction

Groundwater has been extensively used as the only source of pathogen-free drinking water in Bangladesh. Unfortunately, the shallow groundwater in Bangladesh is contaminated with ubiquitous metalloid arsenic (As) and often laden with high As (>50 μg/L, maximum contamination limit for As in Bangladesh) of natural origin [1]. More than 60% of the tested groundwater-wells so far exceeded the current World Health Organization (WHO) provisional guideline value of 10 μg/L [2]. Long-term exposure of arsenic contaminated water can lead to cancer of the liver, lung, kidney, bladder, and skin [3]. Noncancer effects include cardiovascular and cerebrovascular disease, diabetes mellitus, and adversereproductive outcomes. Chronic As poisoning in the As-affected areas in Bangladesh is now widespread and needs immediate measures to provide safe water for at least 20–50 million people [4].

Many options such as household-based filters, low-arsenic dug wells, pond water, sand filters and treatment plants exist to avoid or remove As, but due to the higher cost and maintenance effort the practical and social impediments limit their use [5,6]. Installing deeper wells (>180 m) is a simple solution that does not require extensive infrastructure. Hence, in Bangladesh, the government and different agencies have drilled deep wells without scientific investigation to supply the low-As water to urban and rural populations, where shallow groundwater is contaminated with As [1]. Therefore, it is inevitable to evaluate the details of geochemical processes that govern the chemical composition and quality of deep groundwater in the study area.

Several hypotheses have been proposed to explain groundwater contamination with As in Bangladesh. One of the initially proposed mechanisms of As occurs naturally in sediments due to weathering of arsenopyrite from the Himalayas and subsequent deposition by the Ganges–Brahmaputra–Meghna River system [7]. The current generally accepted explanation for As mobilization is microbial and/or chemical reductive dissolution of As-bearing iron oxyhydroxides in the aquifer sediments [8–10]. Arsenic mobilization in groundwater also appears to be triggered by intensive extraction of groundwater for irrigation and application of phosphate fertilizer [7]. On the other hand, Polizzotto et al. [11] suggested that As is not

* Corresponding author at: Isotope Hydrology Division, INST, Bangladesh Atomic Energy Commission, Savar, GPO Box-3787, Dhaka-1000, Bangladesh.
Tel.: +88 02 7790684; fax: +88 02 8613051.
E-mail address: halim1972@gmail.com (M.A. Halim).

0304-3894/$ – see front matter © 2010 Elsevier B.V. All rights reserved.
doi:10.1016/j.jhazmat.2010.01.008

mobilized within the aquifer but rather in surface soil layers and is subsequently transported down through the sandy aquifer. It is, therefore, evident that As mobilization in Bangladesh groundwater is a complex natural geochemical process.

On the other hand, higher concentrations of boron (B) in water systems are unusual and lead to environmental harm [12]. Boron is a hazard to health in drinking water, so a provisional guideline value of 500 μg/L is quoted by the World Health Organization [13]. Enrichment of boron in water systems can result from hydrothermal influence on infiltrating waters, human pollution, dissolution of evaporates, the presence of residual seawater, and mineral weathering [14]. Moreover, the process of adsorption/desorption of boron to mineral surfaces is an important control on its concentration in waters associated with soils and sediments [15]. In Banglad esh, to the best of our knowledge, except for Ravenscroft and McArthur [14] no other work has yet been done describing the mechanism of regional enrichment of Bengal Delta deep groundwater by boron. Ravenscroft and McArthur [14] has stated that the boron has desorbed from mineral surfaces as freshwater flushing displaces saline waters from the aquifers and the desorption is driven by decreasing ionic strength, the equilibrium readjustment of mineral sorption sites to the low boron concentration in freshwater, and competitive exchange with HCO_3/CO_3. In present study an investigation is carried out with geochemical and geostatistical models to elucidate the spatial distribution, source and release of boron in deep aquifer, which is proposed as an alternative source of As-free drinking water in those areas where high level of As enrichment occurs in shallow aquifer.

Therefore, the main objective of the present paper is to evaluate the geochemical processes that control the release of solutes in deep groundwaters. Special emphasis is put forward to explain the status of As and B in deep groundwaters, their origin and mobility in the deep aquifer, which could be helpful for proper management of deep aquifer as a sustainable source of As-safe drinking water in the study area.

2. Study area

2.1. Location, geology and hydrogeology

The study area covers the southern districts of Bangladesh and geographically, the area is confined within 22.02° to 23.39°N latitudes, and 89.13° to 91.21°E longitudes formed primarily by the deposition of late Holocene to recent sediments carried by the Ganges–Brahmaputra–Meghna rivers (Fig. 1) [10]. The surface lithology is mainly of deltaic and flood plain deposits, which are composed of tidal deltaic deposits, deltaic silt and mangrove swamp deposits [16].

The subsurface geology of the study area has complex interfingerings of coarse and fine-grained sediments from numerous regressions and transgressions throughout geologic time [4]. A generalized stratigraphic section across most of the southern delta reveals alternating sand-dominated and fine-grained sequences. Mineralogy of the floodplain and deltaic sediments is dominated by quartz with some plagioclase and potassium feldspars and volcanic, metamorphic, and sedimentary fragments [17].

In the study area clayey aquitards are present at varying depths [8]. Sands deeper than about 180 m beneath the clayey aquitards are commonly referred to as the 'deep aquifer', which are exploited for potable water supply. Regional scale long-term hydrographs of deep observation wells are not available in Bangladesh and very little information is about the water level behaviors of the deep aquifers. It is perceived that groundwater is under artesian conditions in the deep aquifers. Limited data show that the deeper aquifer water levels also fluctuate annually almost in the same fashion as the shallow groundwater [18].

2.2. Land use and climate

Land use is dominantly agricultural and most of the landmass is made up of fertile deltaic low lands. Maximum elevations are in northwestern region and elevations decrease in the coastal south where the terrain generally at sea level. The study area experiences a tropical monsoon climate and the average annual rainfall varies from 6 to 393 mm with annual total 1850 mm [4]. Up to 85% of the annual rainfall occurs during the May to September monsoon. This coincides with the peak inflow of the major rivers and annual flooding. Less than 5% of the mean annual rainfall occurs during November to March.

3. Methodology

3.1. Sample collection

Deep groundwater samples (depth varying from 180 to 363 m) were collected from 46 domestic wells in the study area during January 2007 to March 2007 (Table 1, Fig. 1). Samples were collected in high-density polypropylene (HDPP) bottles (washed with 1% HNO_3 for 3 times with distilled water before sampling at laboratory and 3 times with well-water before taking the sample) following the procedure outlined by Bhattacharya et al. [19]. Each sample was immediately filtered on site through 0.45 μm filters of cellulose acetate. Filtrate for metals and dissolved organic carbon (DOC) analyses were transferred into polyethylene bottles and immediately acidified with supra pure 7N HNO_3 (Merck, Darmstadt, Germany) for reaching a pH <2 to avoid any precipitation. Samples for anions analyses were collected without acidified. Field blanks (Milli-Q water) were collected to insure the integrity of field sampling methods. All the samples were shipped to Japan and stored in a refrigerator at a temperature of 4 °C until the analysis being performed.

3.2. Field measurements

The physicochemical parameters such as temperature, pH and electrical conductivity (EC) were measured with calibrated portable instruments. The pH Meter (HORIBA Ltd., Japan) was employed to measure pH of groundwater. Electrical conductivity was measured using a Conductivity Meter (HORIBA Ltd., Japan) and temperature was also read from the same meter. The sampled tube wells were actively used and were purged for 10 min prior to measure these parameters. The well locations were determined with a handheld global positioning system (GPS) (Kansas, USA). Alkalinity (as HCO_3^-) was determined by field titration with 1.6N H_2SO_4 to pH ~4.5 using HACH Digital multi Sampler Model 1690. Well depths were noted from the record preserved by the well owners.

3.3. Laboratory measurements

The concentrations of major anions (Cl^-, NO_3^- and SO_4^{2-}) and cations (Na^+, K^+, Ca^{2+} and Mg^{2+}) were measured with ion chromatography (Metrohm 761 Compact IC) in filtered groundwater samples. The instrument was linearly calibrated with standards (Wako Pure Chemicals Industries Ltd., Japan) from 2.5 to 7.5 mg/L. The accuracy and precision of analyses were tested through running duplicate analyses on selected samples. Samples were diluted several times and the relative standard deviation of measured major ions was found to be within ±3%.

The total concentrations of As, boron, Ba, Br, Fe, Mn, Si and Sr were measured by inductively coupled plasma and mass spectrometry (ICP-MS), which was linearly calibrated from 10 to 100 μg/L

Table 1
Hydrogeochemical variables of deep groundwater samples.

Sample ID	Latitude	Longitude	Depth (m)	pH	Temperature (°C)	EC (μS/cm)	HCO_3 (mg/L)	Cl (mg/L)	NO_3 (mg/L)	SO_4 (mg/L)	Br (mg/L)
1	22.79	89.58	267	8.8	28.6	842	448.91	37.92	3.20	0.50	0.27
2	22.95	90.23	363	7.6	24.9	1625	197.01	526.33	6.18	0.55	1.97
3	23.28	90.96	224	7.0	25	2415	169.89	599.35	15.30	0.96	3.47
4	22.73	90.44	302	8.1	26.8	1165	184.68	430.97	8.46	0.59	1.91
5	22.71	90.38	287	8.2	28.5	1605	233.98	603.15	1.21	2.66	4.12
6	22.68	90.39	302	8.2	27.4	425	209.33	47.77	2.45	0.83	0.35
7	22.44	90.44	296	8.4	33.8	555	240.15	9.08	2.79	0.72	0.13
8	22.43	90.36	302	8.2	28.1	605	252.47	6.00	6.91	0.04	0.12
9	23.08	89.84	195	7.3	26.8	2195	338.75	747.94	21.71	0.50	3.56
10	23.31	89.98	210	7.5	26.2	1045	394.21	92.50	18.73	0.60	0.82
11	23.24	90.10	210	7.4	26.7	1805	166.19	686.39	3.73	1.40	3.81
12	22.88	91.22	276	7.0	25.7	1885	98.40	731.10	1.72	36.57	3.97
13	22.43	90.36	241	7.8	27.6	799	258.63	1.97	1.19	0.43	0.11
14	22.12	90.23	314	7.8	29	851	283.28	24.47	1.27	0.36	0.16
15	22.12	90.23	302	7.8	26.7	915	295.61	21.02	2.25	0.12	0.18
16	22.03	90.24	308	7.6	28.3	1025	332.59	34.71	2.86	0.10	0.25
17	21.95	90.18	271	7.7	32.4	1141	344.91	87.85	1.71	0.70	0.50
18	21.91	90.14	297	7.4	28.9	2135	307.94	661.02	3.01	0.01	2.49
19	22.43	90.36	309	8.0	32	732	233.98	11.46	0.95	0.71	0.09
20	22.85	90.25	256	7.7	27.3	1111	160.03	312.02	1.41	0.84	1.24
21	22.80	90.10	241	7.0	24.6	4225	172.36	1670.64	6.52	36.55	6.39
22	23.16	89.51	230	7.0	25.1	1530	241.51	271.39	0.06	3.09	2.21
23	23.17	89.28	340	7.3	26.1	1337	202.07	263.56	0.46	2.10	1.27
24	22.83	89.54	342	7.5	27.2	1548	167.56	326.00	6.29	3.24	2.06
25	22.64	89.80	298	7.4	27.3	2285	179.88	550.39	5.00	1.51	3.38
26	22.49	90.06	290	7.9	26	2391	210.70	615.27	2.83	0.77	4.25
27	22.65	90.18	330	7.9	27.2	1431	216.86	458.32	3.67	0.18	1.36
28	22.73	90.44	290	7.1	27.1	1165	179.88	430.94	8.43	0.56	0.86
29	22.68	90.39	301	8.3	27.6	425	204.53	47.74	2.42	0.80	0.04
30	23.13	89.91	180	7.7	27	1785	364.76	379.55	7.29	0.86	0.91
31	23.18	89.13	342	7.8	27.2	595	210.70	148.99	3.22	0.18	0.81
32	22.75	89.16	330	7.8	27.2	2495	296.97	883.15	14.04	1.45	4.31
33	22.90	89.24	180	7.0	28	1625	155.23	595.29	14.39	1.75	2.89
34	22.81	89.50	300	8.1	29.3	415	161.39	18.65	4.46	3.69	0.16
35	22.66	90.09	270	8.0	27.5	1405	241.51	477.08	8.53	1.32	2.28
36	22.46	90.41	308	8.5	27.5	575	253.83	14.64	2.55	0.61	0.13
37	23.08	89.84	185	7.4	26.9	2195	333.95	747.91	21.68	0.47	3.37
38	23.19	90.19	220	7.5	26.6	1025	155.23	353.28	0.89	0.37	1.53
39	23.39	90.11	262	7.5	27.1	545	161.39	80.55	0.81	3.77	0.39
40	22.59	91.00	290	7.4	27.4	265	99.77	5.68	0.81	0.49	0.05
41	22.77	90.87	301	7.5	27.1	1105	155.23	378.53	2.37	1.83	1.63
42	23.10	89.36	225	7.0	27.6	930	167.56	14.14	1.05	0.08	0.90
43	22.79	89.58	285	7.4	29.4	1411	118.25	503.16	14.88	2.45	1.76
44	23.24	90.10	214	7.3	28.3	2405	155.23	941.84	3.63	0.09	3.74
45	23.23	90.86	245	7.4	29	530	68.95	89.57	0.73	0.13	0.36
46	23.1	91.86	258	7.2	27	307	118.25	7.45	1.05	0.11	0.06

Sample ID	Na (mg/L)	K (mg/L)	Mg (mg/L)	Ca (mg/L)	Ba (μg/L)	Sr (μg/L)	Si (mg/L)	Fe (mg/L)	DOC (mg/L)	As (μg/L)	Mn (μg/L)	B (μg/L)
1	159.70	7.78	9.39	17.17	51.1	171.6	11.75	0.18	1.96	nd	7.2	267
2	523.83	4.14	9.70	21.55	24.4	203.5	11.65	0.50	2.33	3.6	10.6	704
3	336.79	8.63	37.00	41.19	55.8	455.3	16.56	0.66	2.80	32.8	81.7	320
4	526.17	13.62	12.80	31.23	43.0	214.2	7.99	0.23	2.42	0.2	1.9	542
5	534.05	19.11	9.15	15.79	113.3	361.5	9.18	0.51	4.84	nd	4.1	543
6	187.93	5.56	2.77	5.05	6.2	73.46	9.48	0.17	2.55	nd	nd	379
7	181.87	5.23	1.79	3.13	11.2	39.38	9.32	0.16	1.20	nd	5.8	441
8	226.02	8.58	4.42	10.29	17.5	73.35	9.70	0.11	0.65	0.4	nd	424
9	563.55	46.58	58.72	117.73	211.0	561.8	10.40	0.72	5.75	91.1	30.9	429
10	358.31	20.65	26.87	25.57	42.1	190.5	14.93	0.26	2.55	108.8	30.6	439
11	484.30	24.41	42.96	88.10	232.7	726	14.83	0.60	3.10	nd	nd	343
12	450.29	28.53	36.09	44.69	213.2	416.2	28.09	0.57	3.60	nd	8.1	429
13	12.16	7.94	0.70	3.42	10.3	107.2	9.59	0.11	1.26	0.2	10.4	415
14	253.48	10.62	3.99	8.58	11.7	66.43	9.33	0.10	1.48	nd	nd	477
15	280.68	9.67	4.18	8.27	6.9	61.02	9.22	0.29	1.83	0.5	80.3	324
16	315.81	15.55	7.64	12.03	15.2	90.81	9.87	0.22	1.67	5.9	6.7	327
17	345.68	8.73	9.88	16.67	17.2	89.01	9.05	0.40	2.45	1.5	3.8	395
18	580.45	28.97	20.94	25.22	46.1	229.3	9.09	0.57	4.74	nd	26.2	854
19	213.68	6.22	2.24	14.96	12.2	42.34	9.21	0.12	1.67	nd	3.1	392
20	339.10	11.94	5.46	4.42	26.1	91.63	11.47	0.38	2.32	2.0	10.5	624
21	1035.21	77.73	39.55	32.64	367.0	864.9	18.59	0.86	5.01	nd	94.5	1282
22	270.18	7.19	96.22	169.85	783.1	1294	19.54	0.90	5.52	2.1	27.7	267
23	73.26	3.41	39.38	89.28	200.6	488.6	21.00	0.44	1.08	1.2	44.5	234
24	191.97	6.02	34.63	52.01	159.2	520.4	13.84	0.21	1.47	nd	28.9	179
25	499.03	18.38	51.14	120.05	295.3	858.6	12.73	0.50	4.51	0.7	27.2	284
26	357.02	10.39	56.00	84.40	579.2	836.9	8.92	0.48	4.95	2.6	27.8	1113
27	339.86	5.88	4.71	11.08	52.8	129.1	11.07	0.34	2.29	4.9	27.3	797

Table 1 (*Continued*)

Sample ID	Na (mg/L)	K (mg/L)	Mg (mg/L)	Ca (mg/L)	Ba (μg/L)	Sr (μg/L)	Si (mg/L)	Fe (mg/L)	DOC (mg/L)	As (μg/L)	Mn (μg/L)	B (μg/L)
28	526.14	13.59	12.77	31.20	74.6	338.5	18.30	0.26	1.67	nd	32.5	218
29	187.90	5.53	2.74	5.02	210.1	237.1	15.51	0.21	1.59	193.4	28.5	19
30	557.55	28.31	42.23	79.68	103.4	226.5	18.66	0.43	1.12	26.9	27.3	215
31	117.24	10.35	33.06	69.33	78.7	390.2	16.89	0.23	1.85	2.2	29.8	165
32	654.09	27.25	44.25	65.01	503.1	947.8	11.20	0.67	5.45	27.3	34.1	502
33	323.78	23.88	68.42	46.16	481.1	935.7	8.92	0.44	3.21	15.3	26.8	547
34	73.86	7.70	18.18	36.63	130.3	282.9	11.87	0.18	1.47	nd	102.9	131
35	430.80	19.17	13.17	23.12	105.6	239.9	10.26	0.33	2.60	6.0	43.5	1002
36	199.62	5.96	2.84	4.38	27.6	70.3	10.23	0.21	1.02	0.6	30.1	398
37	563.52	46.55	58.69	117.70	252.3	531.9	11.35	0.43	2.74	62.0	46.4	456
38	206.85	17.74	37.94	78.85	213.3	524.1	21.30	0.39	1.19	0.9	27.6	174
39	74.30	10.99	29.08	51.29	105.6	279.2	18.26	0.14	1.27	5.9	31.4	46
40	27.04	5.63	12.43	28.69	64.3	181.7	31.50	0.16	1.10	0.3	27.9	31
41	257.41	14.33	21.74	34.85	115.5	309.2	21.74	0.35	1.51	1.4	27.4	320
42	4.95	1.70	4.60	13.45	141.3	449.2	22.85	0.29	0.77	1.4	26.8	56
43	283.31	26.45	41.63	68.26	164.9	439.1	13.67	0.23	1.32	0.5	30.9	300
44	501.18	24.80	42.59	91.92	213.4	718	16.37	0.55	5.05	0.5	26.3	863
45	45.66	7.11	17.26	42.72	41.6	252.2	32.21	0.19	1.04	0.8	26.5	25
46	30.04	7.26	15.77	28.05	76.0	196.3	34.6	0.12	0.83	0.8	144.7	29

Note: nd is the below detection limit.

with custom multi-element standards (SPEX CertiPrep, Inc., NJ, USA) before use. The relative standard deviation for all measured elements was within ±2%. Triplicate analysis of 10% of all samples and analysis of check standards every 10 samples were performed to assess measurement error, and to check for accuracy and precision of measurement technique. Dissolved organic carbon was measured by high-temperature catalytic oxidation method using a Shimadzu Corp. TOC 5000 analyzer. Detection limit was 0.5 mg/L with a precision of less than ±5%. The analyses were performed at the Center of Advanced Instrumental Analysis, Kyushu University, Japan.

3.4. Statistical analysis

Principal component analysis (PCA) was done on the original data set (without any weighting or standardization) following the theories and methodologies stated by Davis [20] and Dreher [21]. The statistical software package STATISTICA 7 for Windows [22] was used for calculations. After the application of PCA, a varimax normalized rotation was applied to minimize the variances of the factor loadings across variables for each factor. In this study, all principal factors with eigenvalues which are greater than 1.15 are taken into account. The first four factors were able to account for

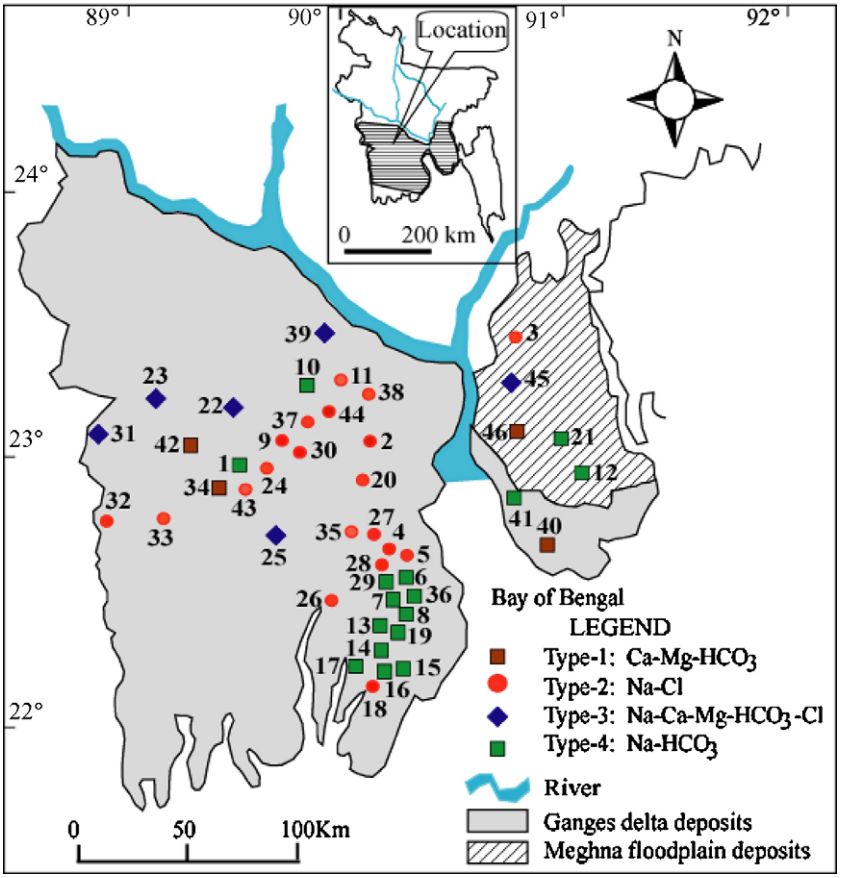

Fig. 1. Location map of the study area and groundwater sampling points.

81.9% of the variance of all variables. The saturation indices were calculated using PHREEQC [23] with thermodynamic database of MINTEQA2 [24]. The Aquachem 4.1 computer code was also used to classify water types. Moreover, geostatistical method variogram is applied to generate four spatial models for distribution of EC, boron, Cl^- and Na^+ [25] for evaluating the source of boron in deep groundwater of Bangladesh.

4. Results and discussion

4.1. Major hydrogeochemical solutes

Physicochemical solutes measured in selected 46-deep groundwater samples and their statistical summary are presented in Tables 1 and 2. The pH values of the assorted groundwater samples vary from 6.9 to 8.8 with average value of 7.6 indicating that the waters are generally neutral to slightly alkaline. The measured water temperatures vary from 24.6 to 33.8 °C with an average of 27.5 °C. Minimum and maximum values of electrical conductivity (EC) are 265.0 and 4225.0 μS/cm with an average value of 1322.3 μS/cm.

The variation of major cations (Na^+, K^+, Ca^{2+} and Mg^{2+}) and anions (Cl^-, HCO_3^-, NO_3^-, Br^- and SO_4^{2-}) concentrations measured in deep groundwater samples is illustrated in the Box and Whisker plot (Fig. 2), where Na^+ and Cl^- are the dominant cation and anion, respectively. Nevertheless, the groundwater samples contained significantly high HCO_3^-. Fig. 2 also shows that the order of relative abundance of major cations in the deep groundwater is $Na^+ > Ca^{2+} > Mg^{2+} > K^+$ (on mg/L basis) while that of anion is $Cl^- > HCO_3^- > NO_3^- > Br^- > SO_4^{2-}$. The electrical conductivity of groundwater samples shows that large percentages of contribution are from Cl^-, Na^+ and HCO_3^-. Since conductivity is a linear function of total dissolved solids (TDS) and for that matter the mineral salt content of groundwater [26].

4.2. Water type

The concentrations of major ions measured in deep groundwater samples are presented in the Piper Trilinear plot (Fig. 3). This figure shows that deep groundwaters in the study area can be broadly divided into four types: Type-1, Ca–Mg–HCO_3; Type-2, Na–Cl; Type-3, Na–Ca–Mg–HCO_3–Cl and Type-4, Na–HCO_3. Twenty-three samples fall in Type-2, while the total of 4, 6 and 13

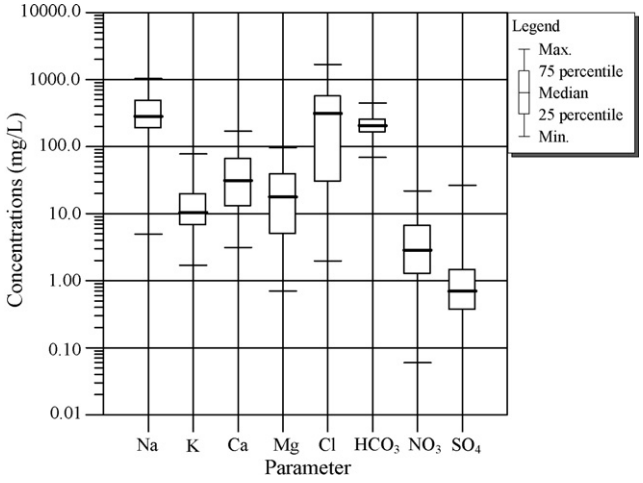

Fig. 2. Box and Whisker plot showing the variation of major ion concentration in the studied deep groundwater samples.

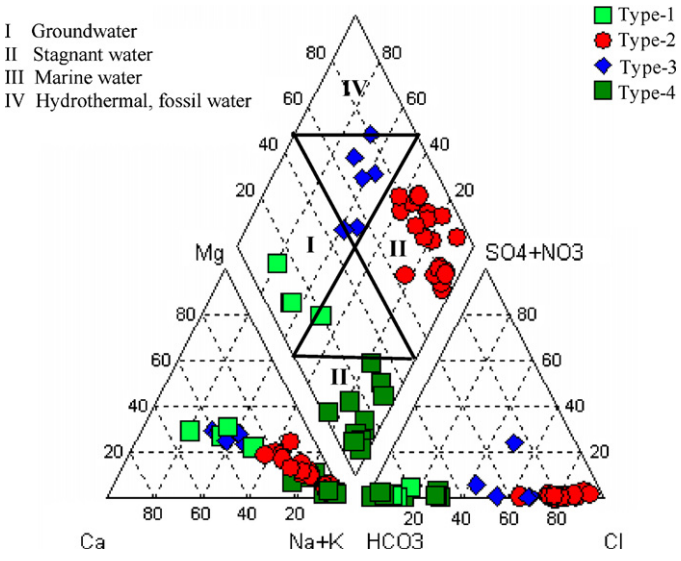

Fig. 3. Piper diagram showing major ion composition of deep groundwaters. The groundwaters are classified into four types; Type-1: Ca–Mg–HCO_3, Type-2: Na–Cl, Type-3: Na–Ca–Mg–HCO_3–Cl and Type-4: Na–HCO_3.

Table 2
Statistical summary of the parameters determined in the deep groundwater samples.

Parameter	Minimum	Maximum	Average	Median	10th	90th	SD	WHO (2004) guideline limit
pH	7.0	8.8	7.6	7.5	7.0	8.2	0.4	6.5–8.5
Temperature (°C)	24.6	33.8	27.6	27.3	25.9	29.2	1.8	
EC (μS/cm)	265	4225	1322	1153	478	2338	780	1500
HCO_3 (mg/L)	69.0	448.9	220.5	206.9	136.7	336.3	82.6	384
Cl (mg/L)	2.0	1670.6	346.7	319.0	10.3	739.5	346.8	250
NO_3 (mg/L)	0.06	21.71	5.33	2.94	0.85	14.64	5.71	50
SO_4 (mg/L)	0.01	36.57	2.56	0.70	0.11	3.17	7.40	250
Br (mg/L)	0.04	6.39	1.67	1.26	0.12	3.89	1.58	
Na (mg/L)	5.0	1035.2	319.7	299.6	59.5	560.5	209.9	200
K (mg/L)	1.7	77.7	15.8	10.5	5.5	28.4	14.0	30
Mg (mg/L)	0.7	96.2	24.9	17.7	2.8	53.6	21.7	150
Ca (mg/L)	3.1	169.9	43.3	31.2	5.0	90.6	38.5	200
Ba (μg/L)	6.2	783.1	145.8	91.0	12.0	331.2	166.7	700
Sr (μg/L)	39.4	1294.0	365.4	265.7	71.8	847.8	295.5	
Si (mg/L)	8.0	34.6	14.8	11.8	9.1	22.3	6.7	
Fe (mg/L)	0.1	0.9	0.4	0.31	0.1	0.6	0.2	0.3
DOC (mg/L)	0.6	5.7	2.5	1.9	1.1	5.0	1.5	
As (μg/L)	0.2	193.4	18.3	2.0	0.4	56.1	40.8	10
Mn (μg/L)	1.9	144.7	32.6	27.6	5.9	76.9	29.0	500
B (μg/L)	18.9	1282.0	407.0	385.5	51.4	825.6	285.4	500

Table 3
Deep groundwater samples with their chemical compositions.

Water type		Sample
Type-1	Ca–Mg–HCO_3	34, 40, 42, 46
Type-2	Na–Cl	2, 3, 4, 5, 9, 11, 12, 18, 20, 21, 24, 26, 27, 28, 30, 32, 33, 35, 37, 38, 41, 43, 44
Type-3	Na–Ca–Mg–HCO_3–Cl	22, 23, 25, 31, 39, 45
Type-4	Na–HCO_3	1, 6, 7, 8, 10, 13, 14, 15, 16, 17, 19, 29, 36

assorted samples belong to Type-1, Type-3 and Type-4, respectively (Table 3). The Ca–Mg–HCO_3 type water occupies the section of the diamond shape in the Piper diagram and their chemical properties dominated by alkaline earths and weak acids [27]. Major groundwaters are of Na–Cl type and they are clustered near the right corner of the central diamond. These waters are of paleo-seawater, connate water or modern seawater [1] while Na–Ca–Mg–HCO_3–Cl type water probably evolved from silicate weathering or ion exchange process [2]. In contrast, the Na–HCO_3 type groundwaters occupy in the lower corner of the central diamond. This type of water may depict rock–water interaction involving the dissolution of carbonate and silicate weathering. Previous hydro-geochemical study of groundwater suggests that meteoric water dissolving Na^+ from Na-bearing silicates would produce Na–HCO_3 water type. Therefore, the incongruent dissolution of albite would probably have produced Na–HCO_3 water type in deep aquifer [28].

4.3. The processes controlling the release of major solutes in deep groundwater

The processes responsible for major solutes in deep groundwater are probably dominated by mineral dissolution as observed by Edmunds et al. [29] in the Midlands aquifer of England. The Cl/∑anions ratios of groundwater samples vary from 0.01 to 0.92 with an average value of 0.54 (Table 4). In contrast, the HCO_3/∑anion ratios change from 0.05 to 0.98 with an average 0.45. These results suggest rock weathering, principally silicate weathering or carbonate dissolution, which has been observed on the Piper plot. The occurrence of Na–HCO_3 water also suggests the possibility of ion exchange. A Na-normalized Ca versus Mg plot (Fig. 4a) and Na-normalized Ca versus HCO_3^- (Fig. 4b) further suggests the deep groundwater samples are influenced by silicate weathering to carbonate dissolution. Therefore, the water chemistry is probably controlled by the carbonate dissolution, cation exchange and silicate weathering and these are discussed below.

Table 4
Summary statistics of saturation indices (SI) of some mineral phases and rations of some chemical constituents in the deep groundwaters.

Parameter	Minimum	Maximum	Average	Median	SD
SI_Calcite	−1.6	1.3	0.1	0.2	0.5
SI_Dolomite	−3.3	2.7	0.2	0.3	1.0
SI_Magnesite	−2.2	0.9	−0.4	−0.3	0.5
SI_Strontianite	−3.4	0.1	−1.4	−1.5	0.6
SI_Anhydrite	−6.2	−2.4	−4.2	−4.2	0.8
SI_Argonite	−1.8	1.2	0.0	0.0	0.5
SI_Barite	−4.2	2.3	−1.7	−1.8	1.3
SI_Quartz	0.4	1.1	0.6	0.6	0.2
SI_SiO_2	−1.4	0.1	−0.4	−0.4	0.2
SI_Siderite	−1.8	1.4	0.1	0.2	0.5
SI_Rhodochrosite	−6.5	−0.1	−1.5	−1.4	1.2
Cl/Br	15.7	1193.4	209.0	182.0	173.6
Cl/∑anion	0.01	0.93	0.54	0.72	0.33
Na/(Na + Cl)	0.30	0.98	0.66	0.59	0.20

4.3.1. Carbonate dissolution

The cations Ca^{2+} and Mg^{2+} often come from carbonate minerals such as calcite and dolomite. Most of the major cations released in groundwater from carbonate minerals dissolution enhanced by respired CO_2 from oxic and anoxic organic matter degradation [10]. Reactions that specifically produce CO_2 through oxidation of organic matter are generalized by:

$$CH_2O(\text{organicmatter}) + O_2 \rightarrow H_2O + CO_2 \quad (1)$$

This reaction is then followed by

$$CaMg(CO_3)_2 + CO_2 + H_2O \rightarrow Mg^{2+} + 2HCO_3^- + CaCO_3 \quad (2)$$

$$CaCO_3 + CO_2 + H_2O \rightarrow Ca^{2+} + 2HCO_3^- \quad (3)$$

resulting in the high Ca^{2+}, Mg^{2+} and HCO_3^- concentrations found in groundwater. There is also CO_2 in rain water which can facilitate carbonate mineral dissolution.

The saturation index of deep groundwater with respect to important carbonate minerals calcite and dolomite was estimated using the hydro-geochemical model PHREEQC [23] with thermodynamic database of MINTEQA2 [24] in order to investigate the level to which the groundwater has equilibrated with these carbonate phases within the sample matrix. The summary statistics of saturated indices of some common mineral phases is presented in Table 4. A plot of calcite saturation index versus dolomite saturation index (Fig. 5) shows that most deep groundwater samples are close to or supersaturated with respect to these minerals. In these samples, super-saturation of carbonate species may result in the preferential precipitation of secondary calcite or dolomite during their transportation into different environments. Previous study [30] indicate that in some of the Himalayan waters, up to

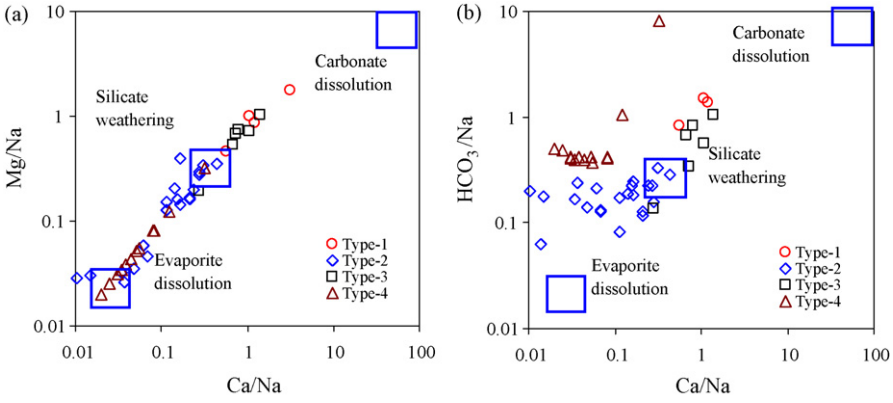

Fig. 4. Molar ratio bivariate plots of (a) Na-normalized Ca and Mg and (b) Na-normalized Ca and HCO_3^-. The boxes represent the ranges of approximate compositions of the three main source end members (evaporate dissolution, silicate weathering and carbonate dissolution) without any mixing.

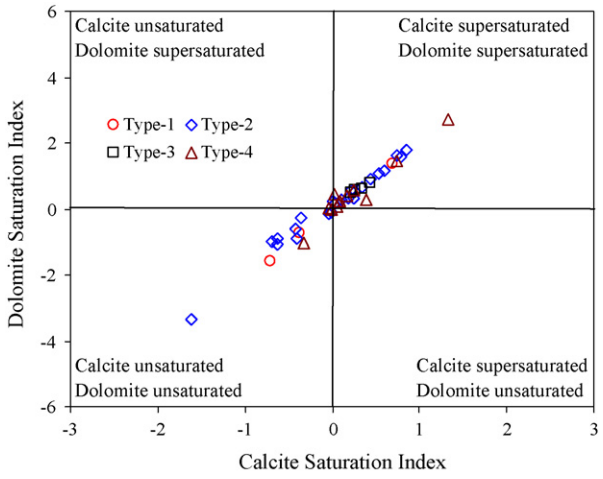

Fig. 5. Relationship between calcite and dolomite saturation indices for all deep groundwater samples analyzed. This plot shows the most waters are supersaturation with respect to calcite and dolomite. A total of 10 samples shows both calcite and dolomite undersaturation.

~70% of Ca^{2+} derived from carbonate dissolution may be removed during transport from the High Himalaya to Lesser Himalaya due to change in water temperature and decreasing of CO_2. On contrary, among the 46 assorted water samples, a total of 10 deep groundwater samples (Type-1: two samples, Type-2: seven samples and Type-4: one sample) are under-saturation with respect to both calcite and dolomite. These samples probably come from an environment where calcite and dolomite are impoverished or where Ca^{2+} and Mg^{2+} exist in other forms and have not reached equilibrium with the carbonates due to short residence time [31]. Moreover, moderate positive correlations ($R^2 = 0.71$ and $R^2 = 0.74$) of Na-normalized Ca with Sr and Ba (Fig. 6a and b) in deep groundwater samples suggests that Sr, Ba and Ca^{2+} have been contributed primarily by carbonate dissolution. Similar results also observed by Mukherjee and Fryar [1] in the deeper groundwaters of the Western Bengal Basin in India.

4.3.2. Seawater intrusion and ion exchange

The deep groundwater samples having $Cl/\sum$anions ratio greater than 0.8 have Na/(Na + Cl) ratio of less than 0.5. The results suggest that they are derived from seawater [32]. In order to ascertain plausibility of the groundwaters being derived from marine origin, chloride to bromide (Cl/Br) ratios of the groundwater samples are measured (Table 4). This ratio (both are in mg/L) close to 300 gives a signature of seawater intrusion [33]. In this study, only four deep groundwater samples (sample #27, 28, 29 and 30) have Cl/Br ratio higher than 300 (337.0, 501.1, 1193.4 and 417.1, respectively). These four sample wells may not be the results of seawater intrusion, but these deep groundwaters are brackish water. These brackish waters are probably results from relict seawater entrapped in the sediments during the Holocene transgression [19]. Besides, Sikdar et al. [34] observed similar type brackish connate water pockets in the western site of Bengal Delta. According to Appelo and Postma [35] when seawater intrudes into fresh coastal aquifer $CaCl_2$ or $MgCl_2$ waters are evolved by the following reactions.

$$2NaCl + CaX = 2NaX + CaCl_2 \quad (4)$$

$$2NaCl + MgX = 2NaX + MgCl_2 \quad (5)$$

where X is the signifies exchanger. In the present study, $CaCl_2$ or $MgCl_2$ water types are not found.

Fig. 7a shows that Na^+ concentrations in most deep groundwaters scattered above the seawater line (slope 0.86) and the excess Na^+ might be the results of cation exchange. In order to investigate the occurrence of cation exchange reaction in the deep groundwaters, Ca + Mg–(HCO_3 + SO_4) (meq/L) is plotted against Na–Cl (meq/L) (Fig. 7b). Since calcite, dolomite, gypsum and anhydrite are the most likely additional sources that Ca^{2+} and Mg^{2+} could enter the groundwater apart from cation exchange. In plotting this diagram, possible contributions of Ca^{2+} and Mg^{2+} from calcite, dolomite, gypsum and anhydrite dissolution to lithogenic Ca^{2+} and Mg^{2+} in the groundwater are accounted by subtracting the equivalent concentrations of HCO_3^- and SO_4^{2-} [36]. Similarly to account for lithologenic Na^+ available for exchange, it is assumed that Na^+ contribution from meteoric origin would be balanced by equivalent concentration of Cl^- and, therefore, equivalent Cl^- concentration is subtracted from that of Na^+ [36]. A negative correlation observed in Fig. 7b suggests that the excess Na^+ in the deep groundwaters due to cation exchange of Na^+ for Ca^{2+} and/or Mg^{2+}.

4.3.3. Silicate weathering

Concentration of Si in the deep groundwater samples varies from 7.99 to 34.6 mg/L with a median value of 11.81 mg/L. Thirty-five samples showed a molar (Na + K)/Cl ratio >1, probably indicating silicate weathering [1]. Possible sources of silica in deep groundwaters include weathering of quartz, feldspars and ferromagnesian silicates. The stability diagrams (Fig. 8) [37] of Ca-silicates and Na-silicates, which are based on solute activities determined by PHREEQC, show the deep groundwaters of study area are in equilibrium with Ca-montmorillonite and Na-montmorillonite, with some samples close to equilibrium with Kaolinite. The reaction involving the incongruent dissolution of

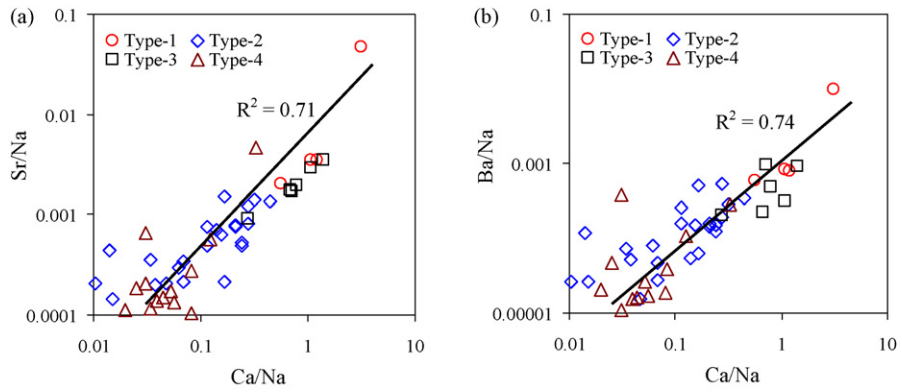

Fig. 6. Bivariate plots showing the relationships between (a) Na-normalized Ca and Sr and (b) Na-normalized Ca and Ba in the deep groundwaters.

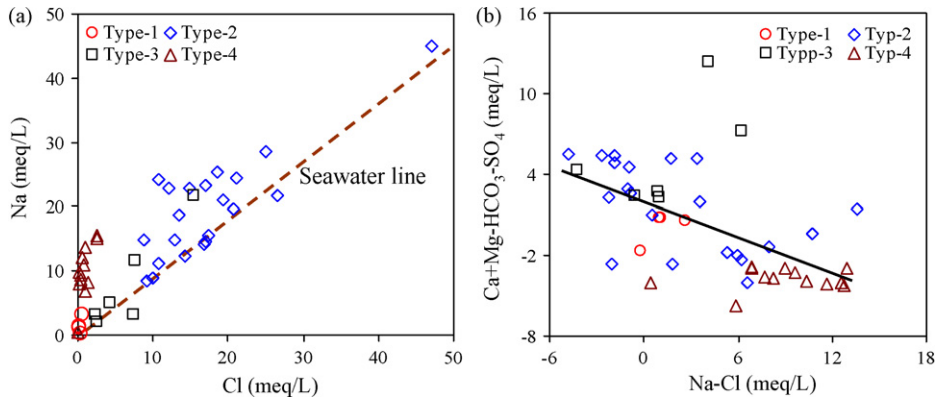

Fig. 7. Bivariate plots showing the relationships between (a) Cl and Na and (b) Na–Cl and Ca + Mg–HCO_3–SO_4 in the deep groundwater samples.

plagioclase (albite) to montmorillonite and kaolinite can be represented by Eqs. (6) and (7), respectively.

$$\underset{\text{Albite}}{2NaAlSi_3O_8} + Mg^{2+} + 4H_2O \rightarrow \underset{\text{Montmorillonite}}{2Na_{0.5}Al_{1.5}Mg_{0.5}Si_4O_{10}(OH)_2} + 2Na^+ + H_4SiO_4 \quad (6)$$

$$\underset{\text{Albite}}{2NaAlSi_3O_8} + H^+ + 9H_2O \rightarrow \underset{\text{Kaolinite}}{Al_2Si_2O_5(OH)_4} + 2Na^+ + 4H_4SiO_4 \quad (7)$$

Montmorillonite is mostly favored in drier climate where the rate of soils flushing is relatively slow [35]. Thus the plotting of the groundwaters in Ca-montmorillonite stability field in Ca–Al silicate phases diagram and in Na-montmorillonite stability field in Na–Cl-silicate phases diagram during the incongruent dissolution of Ca-feldspar (anorthite) and/or Na-feldspar (albite) are consistent with studied deep groundwater samples. These observations match well with what has been observed in most groundwaters in the Accra plains of Ghana [38].

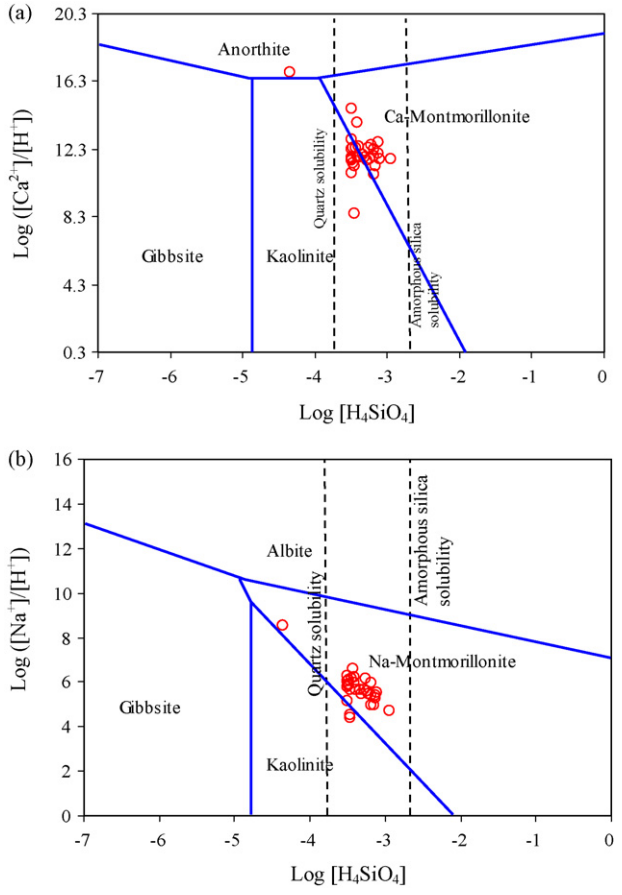

Fig. 8. Stability of (a) Ca–Al silicate phases and (b) Na–Al silicate phases relative to the deep groundwater samples. Phase boundaries are plotted using thermodynamic data of Tardy [37].

4.4. Scenario of arsenic in deep groundwater

The concentration of arsenic (As) in the deep groundwater samples is generally low ranging from <0.05 to 193.4 μg/L with a median value of 1.95 μg/L (Table 2). 17% deep groundwater samples contained As above the WHO guideline [39] for drinking water (<10 μg/L) as well as 8.6% samples (sample #9, 10, 29 and 37 contains As as high as 91.14, 108.8, 193.4 and 61.96 μg/L, respectively) exceeded Bangladesh drinking water standard (<50 μg/L). Most of the recent studies [6,10,13] from the Bengal Basin show that high level of As is present in the shallow aquifer (<100 m) and content of As in groundwater generally decreases with the increase in depth of wells. Several hypotheses have been proposed to explain the As contamination of Bangladesh groundwater. At present the most popular explanation for As mobilization is microbial and/or chemical reductive dissolution of As-bearing iron oxyhydroxides in the aquifer sediments [8–9]. Presence of organic matter in the aquifer sediments of the Bengal Basin has been reported in several studies [8–9,40]. Degradation of this organic matter could drive the sequence of redox reactions in the aquifer and may, thereby enhance As mobilization [8,41–42] and a significant portion of the refractory dissolved organic carbon (DOC) remains for a longer time in the groundwater phase. The concentrations of DOC in the studied samples are low but detectable at all locations and varying from 0.65 to 5.75 mg/L with an median of 1.9 mg/L. Recent studies of Bangladesh groundwater have observed a moderate to strong correlation of DOC with Fe and As, as expected from microbial mediated reductive dissolution of FeOOH with adsorbed As [10,40]. In the present study, elevated level of Fe is observed (ranging from 0.101 to 0.903 mg/L with an median of 0.31 mg/L) and nearly 57% analyzed deep groundwaters have Fe (total) greater than 0.3 mg/L (WHO maximum acceptable limit) (Table 1). Variation in the distribution of As plotted against well depth (Fig. 9a) suggests that content of As in groundwater generally decreases with the increase in depth of wells except for the case of sample #29. In this study, only four samples (sample #9, 10, 29 and 37) out of forty-six have As concentration higher than 50 μg/L (Bangladesh drinking water limit). The previous researchers observed relatively high arsenic concentrations of 57 and 189 μg/L in two deep wells in their study area of Bangladesh [43]. Based on isotopic data they showed that these wells may be screened in both the shallow and the deep aquifers, and concluded the high arsenic contaminated water in the deep wells may be derived preferentially from a shallow depth

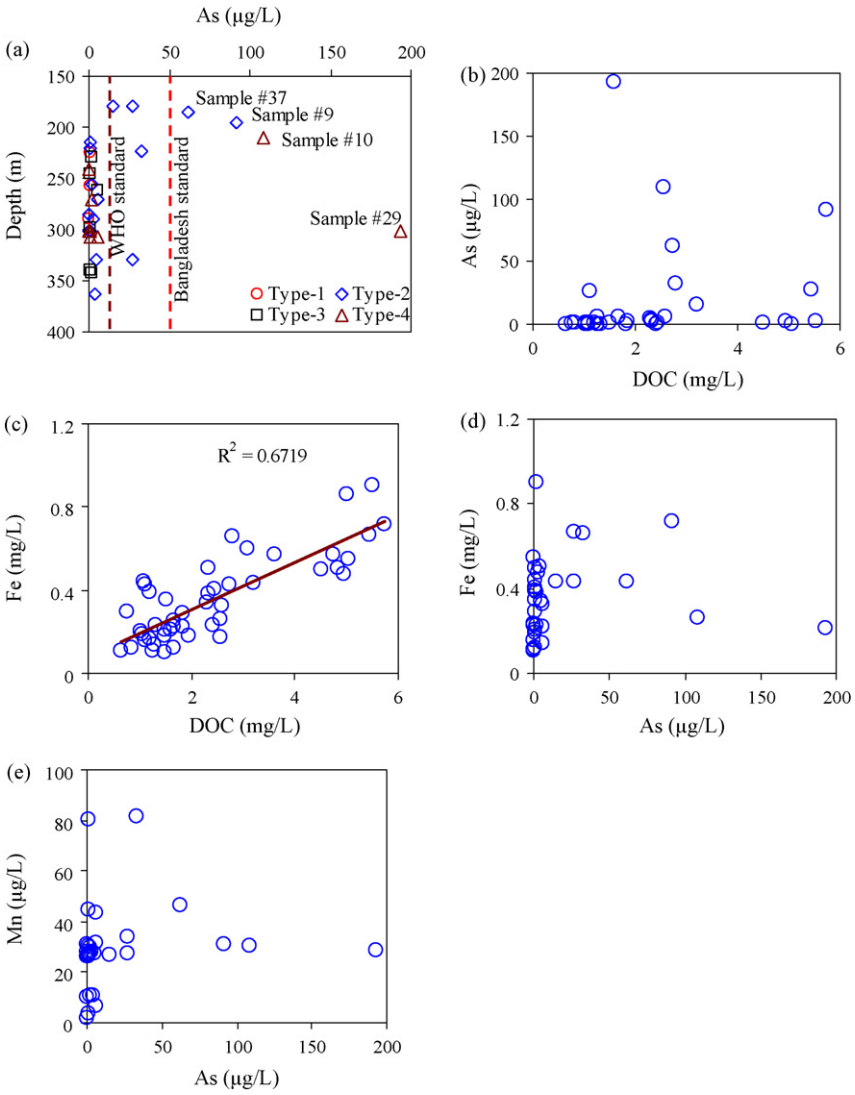

Fig. 9. Bivariate plots showing the relationships between (a) As and depth, (b) DOC and As, (c) DOC and Fe, (d) As and Fe and (e) As and Mn in the deep groundwater samples.

either because of the location of the pump or because of the greater permeability of the shallow aquifers. Thereby we could conclude that four deep wells having elevated concentrations (>50 μg/L) of arsenic may be due to ill-construction of wells and/or due to greater permeability of the shallow aquifers.

The observed As did not correlate with DOC and Fe (Fig. 9b and d), although the correlation between Fe and DOC is strong (R^2 = 0.67, Fig. 9c). Swartz et al. [44] found similar results in their study area of Munshiganj, Bangladesh; where As in sediments of the deeper aquifer (~165 m) does not co-vary with Fe. Such correlations suggest that reduction of Fe and As may not be simultaneous, as suggested by Islam et al. [9]. Moreover, Nickson et al. [13] suggest that some of the As released by reductive dissolution of (Fe/Mn)–OOH can be re-sorbed to the residual or partially reduced metal (oxyhydr) oxides. In this study, As is also not correlated with Mn (Fig. 9e). In contrast, previous researchers have observed correlation of As with Mn [40]. This lack of correlation suggests that no single mechanism can explain As mobilization in the deep aquifer of the study area.

4.5. Scenario of boron in deep groundwater

The concentrations of boron (B) in the study area are ranging from 18.88 to 1282.0 μg/L with an average of 404.97 μg/L (Table 2). Boron concentration in the 26% deep groundwater samples exceeds the WHO standard limits (500 μg/L) for drinking water and all these high content boron samples are of Na–Cl type water (Type-2, Fig. 3). The highest concentration (1282.0 μg/L) of boron is observed in sample #21, which is associated with the largest value of EC (4225 μS/cm). In contrast, all the Ca–Mg–HCO_3 water type (Type-1) contained low boron concentrations (range from 29.03 to 130.8 μg/L with a median of 43.72 μg/L), which also has low values of EC (median of 361 μS/cm). In general, the presence of boron in groundwater depends on its salinity (represented as EC), such that it increases with increasing salinity [45]. Spatial distribution of boron at different depths is shown in Fig. 10a. In this study, a positive correlation between EC and boron (Fig. 10b) suggests that boron might be associated with salinity of these samples. Hence, the salinity mainly reflects the variation of Cl^- concentration, with a strong linear correlation (R^2 = 0.88) between EC and Cl^-, suggesting that the increase of Cl^- concentration contributes to increase in EC value.

Boron exhibits hydrogeochemical retardation in groundwater environments containing a high clay fraction. The hydraulic conductivity, salinity, type of clayey sediments, pH and temperature are the crucial factors that determine boron mobility in the groundwater system [15,46]. Previous hydrochemical studies in Bangladesh indicate that boron in groundwater is principally

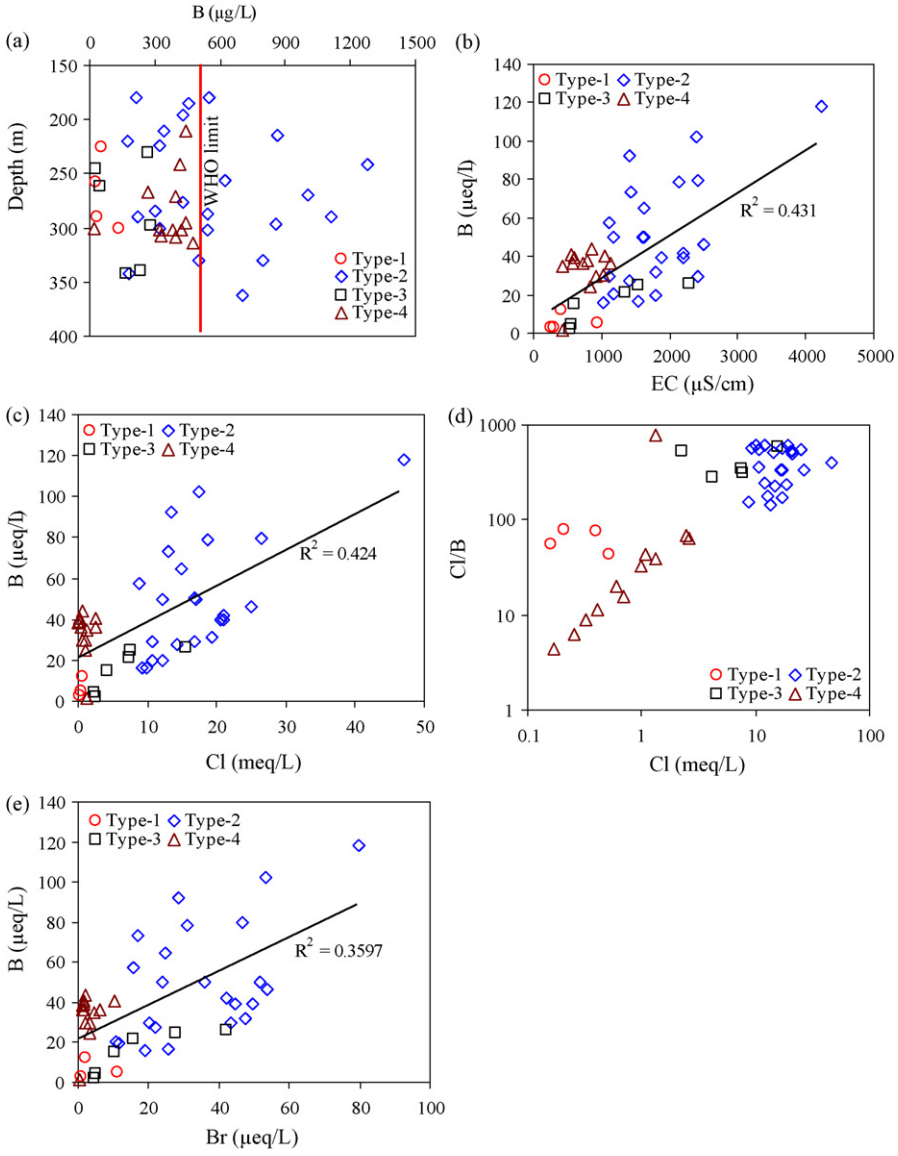

Fig. 10. Bivariate plots showing the relationships of (a) B with depth, (b) EC with B, (c) Cl with B, (d) Cl with B/Cl and (e) Br with B in the deep groundwater samples.

geogenic and appears to drive mainly from residual seawater and/or mineral sorption sites [42]. The positive relationships of boron with Cl^- and Br^- further suggest that boron enrichment in deep groundwater samples might be the result of saline water intrusion (Fig. 10c and e). Moreover, an interesting result can be seen in Fig. 10d, where the molar ratio of boron and Cl^- (B/Cl^-) decrease with increasing Cl^- concentration in the deep groundwaters and all Na–Cl type waters (Type-2) are clustered with high values of Cl^-. As all these wells are deeper than 180 m (Table 1) and comprise private and hand-pumped wells in rural areas, which suggest the presence of brackish water in deep aquifers.

In Bangladesh, deep groundwater moves towards south or southwest [47]. Galy and France-Lanord [48] reported that the Ganges–Brahmaputra Rivers (GBR) sediment load is composed of quartz, clays, primary micas, and carbonates. Most of the sediment is channeled into deeper water through a deep submarine canyon, the Swatch of No Land, creating one of the largest global submarine deltas, the Bengal fan [47]. As observed in the previous section (Fig. 7a), the excess Na^+ in the deep groundwater samples results from the cation exchange of Na^+ for Ca^{2+} due to the deep groundwater flow. A negative correlation between boron and Na normalized

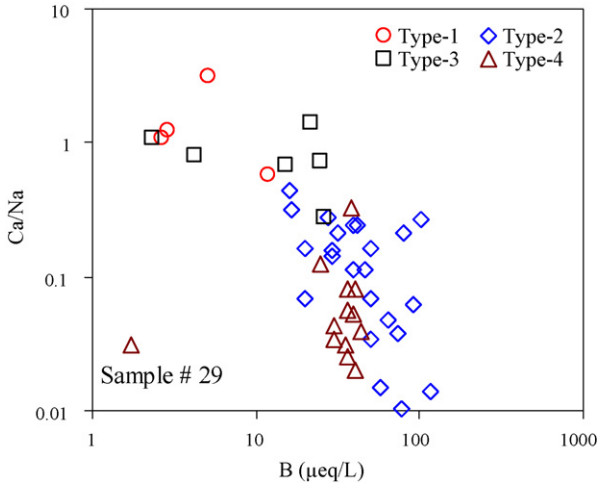

Fig. 11. Bivariate plot showing the relationship of B with Na-normalized Ca in the deep groundwater samples.

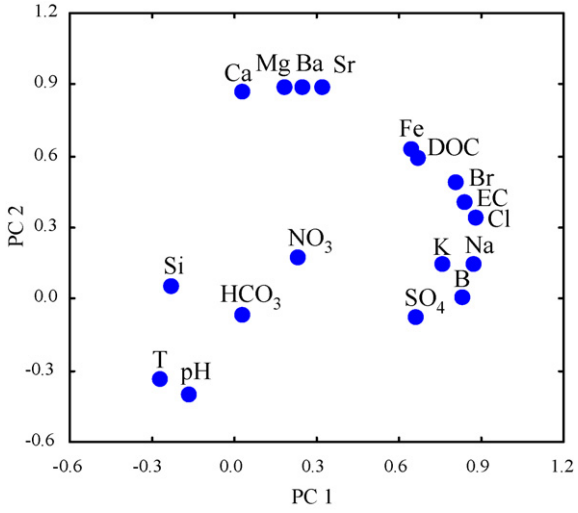

Fig. 12. Principal component analysis based on the hydrogeochemical composition of deep groundwater samples.

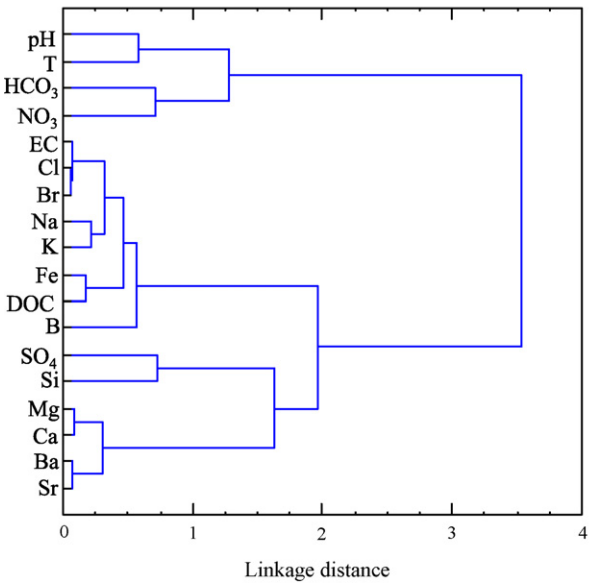

Fig. 13. Cluster analysis based on the hydrogeochemical variables of deep groundwater of the studied area.

Ca in Fig. 11 suggests that enrichment of boron and Na^+ in the deep groundwaters perhaps link to the cation exchange within the clayey sediments, in other words the incomplete flushing in a buried estuary aligned on GBR when they flowed directly south from their present confluence to the Swatch of No Ground canyon [42].

4.6. Multivariate statistical analysis

Principal component analysis (PCA) was applied by considering 18 hydrochemical variables pH, *T*, EC, HCO_3^-, Cl^-, SO_4^{2-}, NO_3^-, Na^+, K^+, Ca^{2+}, Mg^{2+}, Ba, boron, Br^-, Fe, Si, Sr and DOC to all deep groundwater samples. Four PCs extracted using the correlation matrix reflect the processes influencing the chemical composition of groundwater, explaining about 81.9% of total sample variance (Table 5). The variance explanations of the PCs are 48.86%, 16.30%, 10.39% and 6.36% for PC 1, PC 2, PC 3 and PC 4, respectively. In this study, all PCs extracted from the variables were retained with Eigenvalues greater than 1.15. PC 1 is strongly correlated with EC, Cl^-, Br^-, Na^+, K^+, boron, Fe and DOC. On contrary, PC 2 is mainly

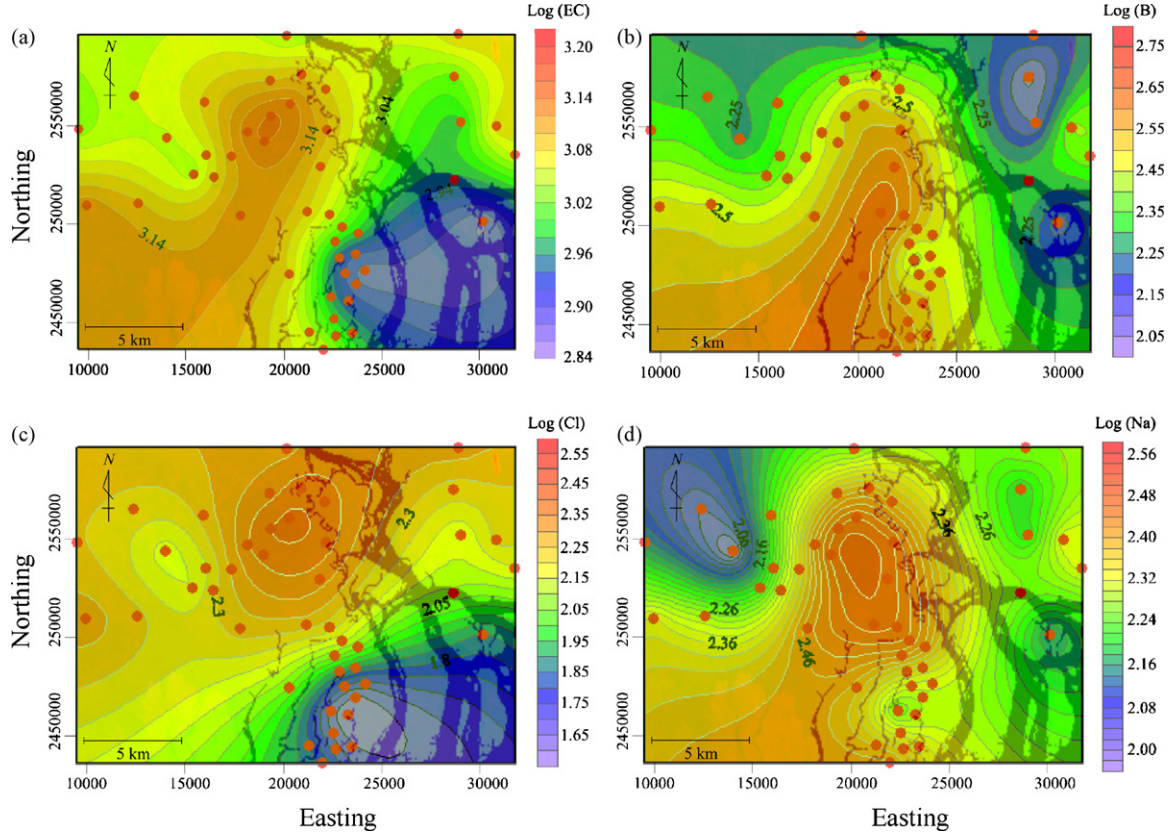

Fig. 14. Results of lognormal kriging (a) EC, (b) B, (c) Cl^- and (d) Na^+ across the study area.

Table 5
Varimax normalized factor loading matrix of 18 physicochemical parameters for groundwater samples.

Parameter	PC 1	PC 2	PC 3	PC 4
pH	−0.17	−0.39	−0.70	−0.26
T	−0.27	−0.33	−0.44	−0.17
EC	0.84	0.41	0.06	0.21
HCO_3	0.02	−0.06	−0.70	0.43
Cl	0.87	0.35	0.17	0.18
NO_3	0.23	0.18	−0.12	0.86
SO_4	0.66	−0.07	0.50	−0.14
Br	0.81	0.50	0.12	0.09
Na	0.87	0.15	−0.11	0.30
K	0.75	0.15	0.15	0.46
Mg	0.18	0.90	0.18	0.27
Ca	0.02	0.88	0.15	0.25
Si	−0.23	0.06	0.87	−0.08
Fe	0.64	0.63	0.11	0.10
DOC	0.66	0.59	−0.20	0.00
B	0.83	0.01	−0.32	−0.12
Ba	0.24	0.89	0.07	−0.11
Sr	0.31	0.90	0.19	0.00
Eigenvalue	8.79	2.93	1.87	1.15
% Variance explained	48.86	16.30	10.39	6.36
% Cumulative variance	48.86	65.15	75.54	81.90

participated Ca^{2+}, Mg^{2+}, Ba and Sr. PC 3 is related to Si and finally PC 4 is contributed by HCO_3^- and NO_3^-. The PCA plot of PC 1 against PC 2 is illustrated in Fig. 12. The PCA plot shows that Fe is strongly correlated to the concentrations of DOC. A significant relationship between EC, Cl^-, Br^-, Na^+, K^+ and boron, and the PC 2 loadings (Ca^{2+}, Mg^{2+}, Ba and Sr) is revealed in the same figure.

Results of cluster analysis (CA) performed in Ward's mode by STATISTICA 7.0 for Windows StatSoft Inc. Statistica [22] and using the physicochemical parameters of all deep groundwater samples are presented in Fig. 13. Several common features are observed in this plot, and these are very similar to that examined in PCA and previous sections. The cluster made in Mg^{2+}, Ca^{2+}, Ba and Sr join with the cluster of Si and SO_4^{2-} further suggests the silicate weathering is one of the processes to release these cations in the deep groundwater. Similarly, EC is formed strong cluster with Cl^-, Br^- and Na^+, which indicates the influence of seawater and they are inter-related and linked to boron. Moreover, Kriging method is adopted to estimate the spatial distribution of EC, boron, Cl^- and Na^+ in the deep groundwater samples. The variogram components of the model are used as input parameters for Kriging. The final results are shown by contour map in Fig. 14. The outputs of this geostatistical approach further suggest the enrichment of boron in deep groundwater might be the results of brackish water.

5. Conclusions

This paper focuses on the hydrogeochemistry of deep groundwater (depth varies from 180 to 362 m with a median of 288.3 m) in Bangladesh to evaluate the arsenic safe drinking water resources. The hydrogeochemical composition of deep wells in the study area show that the groundwater is generally near neutral (median of pH is about 7.5) with few of the wells showing mildly basic character. The Na^+ is the predominant cation in deep aquifer while Cl^- and HCO_3^- are the major anions. Four water types Ca–Mg–HCO_3, Na–Cl, Na–Ca–Mg–HCO_3–Cl and Na–HCO_3 are identified using the Piper diagram and among them, Na–Cl is the principal groundwater. The Na–Cl deep groundwaters are probably connate water from the proto-Bay of Bengal, which has been modified by diagenetic processes and recharge from the shallow aquifer. The deep groundwaters are generally supersaturated with respect to major carbonate species namely calcite and dolomite. Carbonate dissolution and cation exchange are the dominant hydrogeochemical processes controlling the major ions in the deep groundwater, but silicate weathering is also playing an important role.

The main source of elevated level of Fe (around 57% study samples have exceeded the WHO guide line of 0.3 mg/L) in the deep groundwater is reductive dissolution of Fe-oxyhydroxide in the presence of organic matter and this high concentration of Fe is removed through the use of aerators or iron-removal plants. Generally, arsenic concentration in the deep groundwaters is low ranging from <0.05 to 193.4 μg/L with an median value of 1.95 μg/L. Approximately 17% of the deep wells have As concentration exceeding the WHO's maximum acceptable limit of 10 μg/L for drinking water as well as around 8% deep groundwaters exceeded Bangladesh drinking water standard of 50 μg/L. This percentage (8%) of contaminated deep wells is relatively lower because, most of the shallow wells of this study area are highly contaminated with As. No correlation of As with Fe and DOC is observed and this lack of correlation suggests that no single mechanism can explain As mobilization in the deep aquifer of the present study area.

The median value of boron in the deep groundwaters is around 404 μg/L, with the highest concentration (1282 μg/L) of boron is observed in the Na–Cl water type, which is associated with the greatest value of EC (4225 μS/cm). The concentration of boron in about 26% deep wells exceeded the WHO standard limit (500 μg/L) for drinking water. In this study, the positive relationships of boron with Cl^- and Br^- suggest that boron enrichment may be the results of paleo-seawater/connate water trapped in the deep aquifers sediment. Secondly, a negative relationship between boron and Na-normalized Ca suggests cation exchange might be another process to release boron and Na^+ in deep groundwater. Finally, based on this study, recommendation has been made to the local authorities to control the use of deep groundwater only for drinking purpose and need for regular monitoring to ensure sustainable safe use of the resource.

Acknowledgements

The first author would like to acknowledge the Japan Society for the Promotion of Science (JSPS) for financial support through the research grant 18-06396/2006–2007 on the simulation and remediation model for the groundwater contaminated by arsenic and multi-geochemical species. The authors wish to thank Dr. Watanabe, Center of Advanced Instrumental Analysis, Kyushu University, Japan, for her kind support in providing necessary laboratory facilities to analysis groundwater samples. We are grateful to Dr. Delwar Hossain, Jahangirnagar University for his kind support during manuscript preparation. The authors are also pleased to thank Dr. Gerasimos Lyberatos and two anonymous reviewers for their thoughtful, constructive and very useful comments, which improved the quality of the manuscript.

References

[1] A. Mukherjee, A.E. Fryar, Deeper groundwater chemistry and geochemical modeling of the arsenic affected western Bengal basin, West Bengal, India, Appl. Geochem. 23 (2008) 863–894.
[2] M.A. Hasan, K.M. Ahmed, O. Sracek, P. Bhattacharya, M. von Bromssen, S. Broms, J. Fogelstrom, M.L. Mazumder, G. Jacks, Arsenic in shallow groundwater of Bangladesh: investigations from three different physiographic settings, Hydrogeol. J. 15 (2007) 1507–1522.
[3] C. Liao, T. Lin, S. Chen, A Weibull-PBPK model for assessing risk of arsenic-induced skin lesions in children, Sci. Total Environ. 392 (2008) 203–217.
[4] D.G. Kinniburgh, P.L. Smedley (Eds.), BGS and DPHE, Arsenic Contamination of Groundwater in Bangladesh, vol. 2, Tech. ReportWC/00./19, British Geological Survey, 2001, 267 pp.
[5] B.A. Hoque, M.M. Hoque, T. Ahmed, S. Islam, A.K. Azad, N. Ali, M. Hossain, M.S. Hossain, Demand-based water options for arsenic mitigation: an experience from rural Bangladesh, Public Health 118 (2004) 70–77.

[6] A. Milton, W. Smith, K. Dear, J. Ng, M. Sim, G. Ranmuthugala, K. Lokuge, B. Caldwell, A. Rahman, H. Rahman, A. Shraim, D. Huange, M.A. Abrar, Randomised intervention trial to assess two arsenic mitigation options in Bangladesh, Epidemiology 17 (2006) S219.
[7] S.K. Acharyya, P. Chakraborty, S. Lahiri, B.C. Raymahashay, S. Guha, A. Bhowmik, Arsenic poising in the Ganges Delta, Nature 401 (1999) 545.
[8] R.T. Nickson, J.M. McArthur, P. Ravenscroft, W.G. Burgess, K.M. Ahmed, Mechanism of arsenic release to groundwater, Bangladesh and West Bengal, Appl. Geochem. 15 (2000) 403–413.
[9] F.S. Islam, A.G. Gaultm, C. Boothman, D.A. Polya, J.M. Charnock, D. Chatterjee, J.R. Lloyd, Role of metal-reducing bacteria in arsenic release from Bengal Delta sediments, Nature 430 (2004) 68–71.
[10] M.A. Halim, R.K. Majumder, S.A. Nessa, Y. Hiroshiro, M.J. Uddin, J. Shimada, K. Jinno, Hydrogeochemistry and arsenic contamination of groundwater in the Ganges Delta Plain, Bangladesh, J. Hazard. Mater. 164 (2009) 1335–1345.
[11] M.L. Polizzotto, C.F. Harvey, G.C. Li, B. Badruzzman, A. Ali, M. Newville, S. Sutton, S. Fendorf, Solid-phases and desorption processes of arsenic within Bangladesh sediments, Chem. Geol. 228 (2006) 97–111.
[12] A. Vengosh, C. Helvaci, I.H. Karamanderesi, Geochemical constraints for the origin of thermal waters from western Turkey, Appl. Geochem. 17 (2002) 163–183.
[13] WHO, Guidelines for Drinking Water Quality, second ed., World Health Organization, Geneva, Switzerland, 1998.
[14] P. Ravenscroft, J.M. McArthur, Mechanism of regional enrichment of groundwater by boron: the examples of Bangladesh and Michigan, USA, Appl. Geochem. 19 (2004) 1413–1430.
[15] S. Goldberg, H.S. Forster, E.L. Heick, Boron adsorption mechanisms on metal oxides, clay-minerals, and soils inferred from ionic-strength effects, Soil Sci. Soc. Am. 57 (1993) 704–708.
[16] M. Alam, Bangladesh in World Regional Geology, Columbia University Press, New York, 1990.
[17] A. Uddin, N. Lundberg, A paleo-Brahmaputra, subsurface lithofacies analysis of Miocene deltaic sediments in the Himalayan–Bengal system, Bangladesh, Sediment. Geol. 123 (1998) 239–254.
[18] Y. Zheng, S. Datta, M. Stute, R. Dhar, M.A. Hoque, M.W. Rahman, K.M. Ahmed, P. Schlosser, A. van Geen, Stable isotopes (^{18}O, ^{2}H) and arsenic distribution in the shallow aquifers in Araihazar, Bangladesh, Eos Transactions American Geophysical Union, 86 (52), Fall Meeting Supplement, Abstract H31B-1305, 2005.
[19] P. Bhattacharya, G. Jacks, K.M. Ahmed, A.A. Khan, J. Routh, Arsenic in groundwater of the Bengal Delta Plain aquifers in Bangladesh, Bull. Environ. Contam. Toxicol. 69 (2002) 538–545.
[20] J.C. Davis, Statistics and Data Analysis in Geology, John Wiley and Sons, New York, 1986.
[21] T. Dreher, Evaluation of graphical and multivariate methods for classification of water chemistry data, Hydrogeol. J. 11 (2003) 605–606.
[22] StatSoft Inc. STATISTICA (Data Analysis Software System), Version 7, 2006.
[23] D.L. Parkhurst, C.A.J. Appelo, Users Guide to PHREEQC (version 2): A Computer Program for Speciation, Batch-reaction, One-dimensional transport, and Inverse Geochemical Modeling, US Geological Survey Water Resources Investigation Report, 1999, pp. 99–4259.
[24] J.D. Allison, D.S. Brown, K.J. Novo-Gradac, MINTEQA2/PRODEFA2A Geochemical Assessment Model for Environmental Systems Version 3.0 User's Manual, Environmental Research Laboratory, Office of Research and Development, U.S. Environmental Protection Agency, Athens, Georgia, 1990.
[25] H. Wackernagel, Multivariate Geostatistics: An Introduction with Applications, 2nd ed., Springer-Verlag, Heidelberg, German, 2003.
[26] B.K. Kortatsi, Hydrochemical characterization of groundwater in the Accra plains of Ghana, Environ. Geol. 50 (2007) 299–311.
[27] K.R. Karanth, Groundwater Assessment Development and Management, Tata McGraw-Hill Publishing Company Limited, New Delhi, 1994 (third reprint).
[28] R.M. Garrels, F.T. Mackenzie, Origin of the chemical compositions of some springs and lakes, in: R.F. Gound (Ed.), Equilibrium Concepts in Natural Water Systems, American Chemical Society Publications, Washington, DC, 1967.
[29] W.M. Edmunds, A.H. Bath, D.L. Miles, Hydrochemical evolution of the East Midlands Triassic sandstone aquifer, England, Geochim. Cosmochim. Acta 46 (1982) 2069–2081.
[30] M.J. Bickle, H.J. Chapman, J. Bunbury, N.B. Harris, W. Fairchild, T. Ahmed, C. Pomies, Relative contribution of silicate and carbonate rocks to riverine Sr fluxes in the headwaters of the Ganges, Geochim. Cosmochim. Acta 69 (2005) 2221–2240.
[31] D. Langmuir, Aqueous Environmental Geochemistry, Prentice Hall, Upper Saddle River, 1997.
[32] A.W. Hounslow, Water Quality Data Analysis and Interpretation, Lewis Publishers, Boca Raton, 1995.
[33] E. Mazor, Interpretation of environmental isotope and hydrochemical data in groundwater hydrology, in: Proceedings of an Advisory Group Meeting, Vienna, International Atomic Energy Agency, Vienna, Austria, 27–31 January 1975, 1976.
[34] P.K. Sikdar, S.S. Sarkar, S. Palchoudhury, Geochemical evolution of groundwater in the Quarternary aquifer of Calcutta and Howrah, India, J. Asian Earth Sci. 19 (2001) 579–594.
[35] C.A.J. Appelo, D. Postma, Chemical Analysis of Groundwater, Geochemistry, Groundwater and Pollution, Balkema, Rotterdam, 1999.
[36] H. Nkotagu, The groundwater geochemistry in a semi-arid, fractured crystalline basement area od Dodoma, Tanzania, J. Afr. Earth Sci. 23 (1996) 593–605.
[37] Y. Tardy, Characterization of the principal weathering types by the geochemistry of waters from some European and African crystalline massifs, Chem. Geol. 7 (1971) 253–271.
[38] B.K. Kortatsi, Hydrochemical characterization of groundwater in the Accra plains of Ghana, Environ. Geol. 50 (2006) 299–311.
[39] WHO, Guidelines for Drinking Water Quality Recommendations, vol. 1, World Health Organization, Geneva, Switzerland, 2004, 515 pp.
[40] K.M. Ahmed, P. Bhattacharya, M.A. Hasan, S.H. Akhter, S.M.M. Alam, M.A.H. Bhuyian, M.B. Imam, A.A. Khan, O. Sracek, Arsenic enrichment in groundwater of the alluvial aquifers in Bangladesh: an overview, Appl. Geochem. 19 (2004) 181–200.
[41] M.H. Anawer, J. Akai, K. Komaki, H. Terao, T. Yoshimura, T. Ishizuka, S. Safiullah, K. Kato, Geochemical occurrence of arsenic in groundwater of Bangladesh: sources and mobilization processes, J. Geochem. Explor. 77 (2003) 109–131.
[42] P. Ravenscroft, W.G. Burgess, K.M. Ahmed, M. Burren, J. Perrin, Arsenic in groundwater of the Bengal basin, Bangladesh: distribution, field relations, and hydrogeologic setting, Hydrol. J. 13 (2005) 727–751.
[43] P.K. Aggarwal, A.R. Basu, R.J. Poreda, K.M. Kulkarni, K. Froehlich, S.A. Tarafdar, M. Ali, N. Ahmed, A. Hussain, M. Rahman, S.R. Ahmed, A report on isotope hydrology of groundwater in Bangladesh: implications for characterization and mitigation of arsenic in groundwater, IAEA—TC Project (BGD/8/016), 2000.
[44] C.H. Swartz, N.K. Blute, B. Badruzzman, A. Ali, D. Brabander, J. Jay, J. Besancon, S. Islam, H.F. Hemond, C.F. Harvey, Mobility of arsenic in a Bangladesh aquifer: inferences from geochemical profiles, leaching data, and mineralogical characterization, Geochim. Cosmochim. Acta 68 (2004) 4539–4557.
[45] A. Arad, U. Kafri, L. Halicz, I. Brenner, Genetic identification of the saline origins of groundwaters in Israel by means of minor elements, Chem. Geol. 54 (1986) 251–270.
[46] A. Vengosh, A. Starinsdy, Y. Kolodny, A.R. Chivas, Boron isotope geochemistry as a tracer for the evolution of brines and associated hot springs from the Dead Sea, Israel, Geochimi. Cosmochimi. Acta 55 (1991) 1689–1695.
[47] C.B. Dowling, R.J. Poreda, A.R. Basu, S.L. Peters, P.K. Aggarwal, Geochemical study of arsenic release mechanisms in the Bengal Basin groundwater, Water Resour. Res. 38 (2002) 1173–1190.
[48] A. Galy, C. France-Lanord, Weathering processes in the Ganges-Brahmaputra basin and the riverine alkalinity budget, Chem. Geol. 159 (1999) 31–60.